



Project no. TIP5-CT-2006-0314150

INNOTRACK

Integrated Project (IP)

Thematic Priority 6: Sustainable Development, Global Change and Ecosystems

D4.4.3 - Evaluation of an Inspection Demonstrator (Phase 2: Track Tests)

Due date of deliverable: 31st July 2009

Actual submission date: 4th September 2009

Start date of project: 1 September 2006

Duration: 36 months

Organisation Name of lead contractor for this deliverable:

University of Birmingham

Revision Final

Project co-funded by the European Commission within the Sixth Framework Programme (2002-2006)		
Dissemination Level		
PU	Public	X
PP	Restricted to other programme participants (including the Commission Services)	
RE	Restricted to a group specified by the consortium (including the Commission Services)	
CO	Confidential, only for members of the consortium (including the Commission Services)	

Table of Contents

Glossary	2
Executive Summary	3
1. Introduction	4
1.1 Background	4
1.2 Test Site	4
2. Inspection of Surface Defects by ACFM	6
2.1 Background	6
2.2 Initial Laboratory Tests	7
2.3 On-site Testing	12
2.4 Conclusions	14
3. Detection of Surface Defects by Image Analysis	15
3.1 Background	15
3.3 Conclusions	18
4. Inspection of Surface Defects by EMATs	19
4.1 Background	19
4.2 On-Site Testing	19
4.3 Conclusions	21
5. Conclusions	22
6. References	24

Glossary

ACFM	Alternating Current Field Measurement
ECP	Electric Current Perturbation Method
EMATs	Electromagnetic Acoustic Transducers
FFT	Fast Fourier Transform
PoD	Probability of Detection
RCF	Rolling Contact Fatigue

Executive Summary

Within SP4.4, work to date has focussed on:

1. A review of the state-of-the-art in non-destructive testing for railway track and elicitation of requirements for further operational improvements (D4.4.1);
2. Further research and development of new techniques that have the potential to fulfil the identified operational requirements (D4.4.2).

This report builds on the previous work by providing details of the experimental trials that were undertaken on an operational track to ascertain the practical difficulties of migrating lab based technology to a working railway.

In June 2009, during a non-traffic possession on Network Rail's Great Western Route, two specially developed test trolleys were used to re-inspect previously identified light and moderate rolling contact fatigue defects. During the trials three different approaches were investigated:

- ACFM - Alternating Current Field Measurement (undertaken by University of Birmingham – Trolley 2 – see Section 2);
- Vision based inspection (undertaken by Corus – Trolley 1 – see Section 3);
- EMATs - Electromagnetic Acoustic Transducers (undertaken by University of Warwick and University of Birmingham – Trolley 2 – see Section 4).

1. Introduction

1.1 Background

Rail defects, such as rolling contact fatigue (head checks and squats) and wheel burns, are visible on the surface of the rail. The location and shape of the running band is also visible, giving information on defects and features, such as corrugation and welds. Current inspection techniques require maintenance staff to patrol sections of track at regular intervals and report the location of defects as well as certain characteristic features. Rolling contact fatigue (RCF) cracks are an example whereby the surface features can relate to the severity of the defect. Through metallurgical examination of many rail samples, a relationship between the surface crack length and depth has been found, as shown in Figure 1.1. This relationship is used by Network Rail to categorise the severity of defects and plan the maintenance required. The relationship can be summarised in that surface cracks of less than 20mm correspond to crack depths of less than 5mm. If cracks are allowed to grow to surface crack lengths of greater than 20mm, the crack depth can be much greater than 5mm and become difficult to control by grinding. This relationship has been derived from studies of R220 grade, the work carried out in WP4.1 and WP4.3 indicate that the relationship is actually a function of rail grade although further work is required to confirm this[1A, 1C].

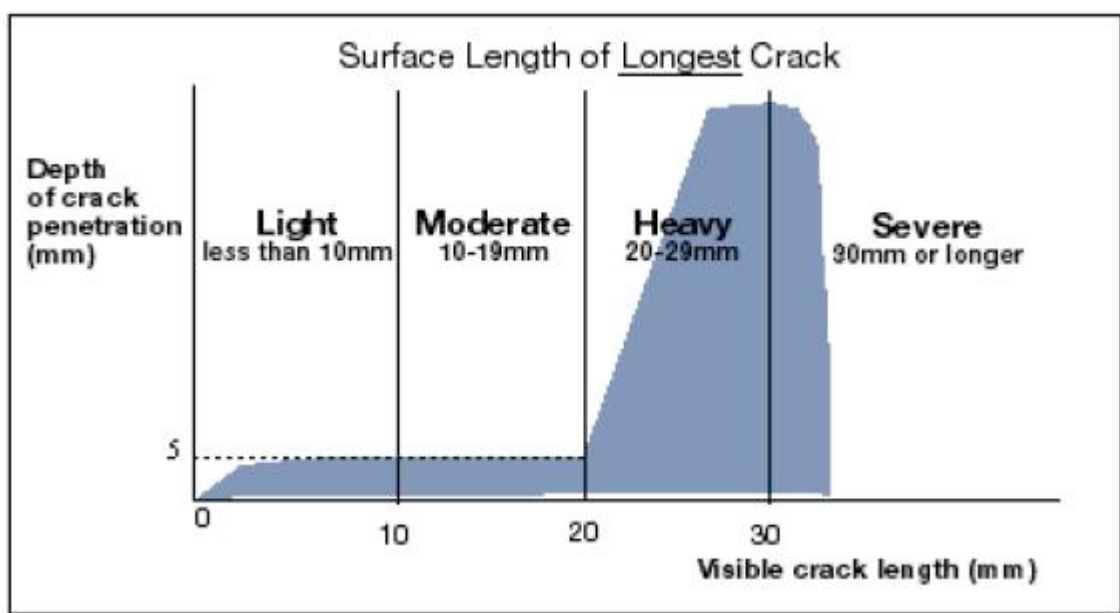


Figure 1.1 - Relationship between surface crack length and depth of RCF cracks [1C]

As the current inspection method is manual, categorisation is only carried out for the most severe defects at each location and relies on an approximation of location and severity. Through the application of automated inspection technology, it is possible to readily detect and characterise these types of surface defects automatically as well as position them more accurately.

1.2 Test Site

Two rail sections, each approximately 20 m long, were inspected during the Swindon tests. The first section was identified as containing light RCF cracks, while the second was identified as containing moderate RCF

cracks during ultrasonic testing and visual inspection conducted by Network Rail,. The tracks were ground prior to the inspection trials as shown in Figure 1.2.

The rail at the site was grade R220 (the rail branding identified the rail to be BS11: 1959 open hearth basic grade produced by Colvilles Ltd. in 1968).



Figure 1.2 - Photograph showing the quality of the surface of the rail sections inspected during the Swindon trials

2. Inspection of Surface Defects by ACFM

2.1 Background

The ACFM (Alternating Current Field Measurement) technique, also known as Electric Current Perturbation (ECP) method, is based on the principle that an alternating current can be induced to flow in a thin skin near the surface of any conductor. When a remote uniform current is introduced into an area of the component under test, if there are no defects present, the electrical current will be undisturbed. If a crack is present the uniform current is disturbed and the current flows around the ends and down the faces of the crack. Because the current is an alternating current, it flows in a thin skin close to the surface and is unaffected by the overall geometry of the component.

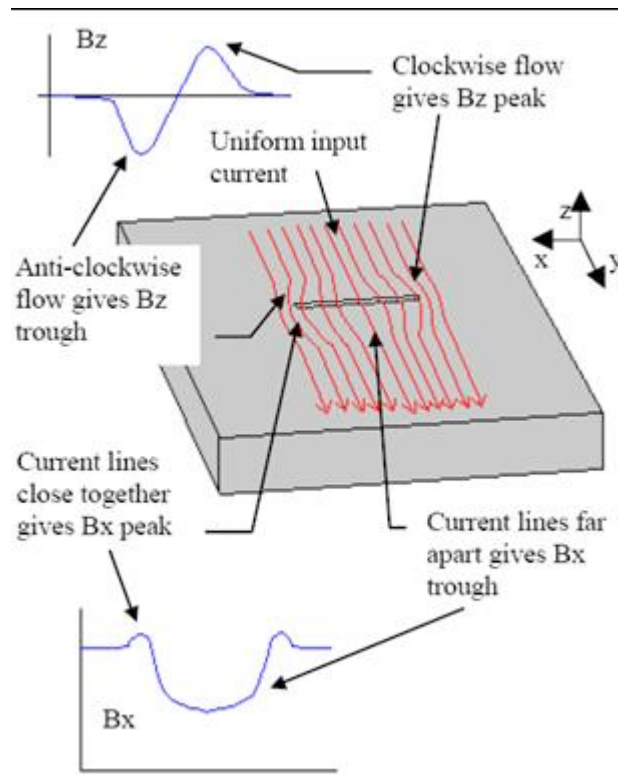


Figure 2.1 - Definition of field directions and co-ordinate system used in ACFM

Associated with the current flowing in the surface is a magnetic field above the surface which, like the current, will be disturbed if a defect is present. An important factor of the ACFM technique is its ability to relate measurements of the magnetic field disturbance to the size of defect that caused that disturbance. The development of the method came from a combination of research studies, which provided mathematical modelling of the magnetic field rather than electrical fields, and advances in electronics and sensing technology [2-10].

The magnetic field above the surface is a complex three-dimensional field. However, by choosing suitable orthogonal axes it is possible to measure components of the field that are indicative of the nature of the disturbance and which can be related to the physical properties of any cracks present. Figure 2.1 presents a plan view of a surface breaking crack where a uniform AC current is flowing. The field component denoted by B_z corresponds to the poles generated as the current flows around the ends of the crack, introducing current rotations in the plane of the component. These responses are principally at the crack ends and are indicative of crack length. The field component denoted by B_x corresponds to the reduction in current

surface density as the current flows down the crack and is indicative of the depth of the defects. Generally, the current is introduced perpendicular to the expected direction of cracking. In practice, special probes have been developed which contain a remote field induction system to introduce the field into the component. This is done together with special combined magnetic field sensors that allow accurate measurement of the components of the magnetic field at the same point in space. The probe requires no electrical contact with the component and can therefore be applied without the removal of surface contaminants.

ACFM probes are available as standard pencil probes and multi-element array probes. These probes can be customised to optimise inspection of particular structural components and maximise the Probability of Detection (PoD) of critical-sized defects. ACFM pencil probes can detect surface-breaking defects in any orientation. Nonetheless, in order to size defects, they need to lie between 0°-30° to the direction of travel of the probe. This drawback is overcome in ACFM arrays by incorporating various field inducers to allow a field to be introduced within the inspected surface in other orientations. This is particularly useful in situations where the crack orientation is unknown or variable. In this case, additional sensors, denoted by B_y, are also incorporated in order to take full advantage of the additional input field directions.

2.2 Initial Laboratory Tests

To make best use of an ACFM array probe, it is necessary to switch through the sensors as quickly as possible in order to allow rapid inspection. However, there are inherent limitations to this including switching settling times, data transfer rates and limitations in the sampling of a 5 kHz signal. With conventional analogue electronics these factors limit the speed of scan for array probes to around 0.5 km/h for a single field 16-channel array. By increasing the energising frequency from 5 kHz to 50 kHz and the sampling rates to 50 kHz, together with modifications to the signal processing electronics, ACFM array systems can achieve scanning speeds of ~3 km/h.

Tests up to 121.5 km/h carried out using a turning lathe test rig have shown the potential of the ACFM technique for high-speed rail inspection. A high-speed micro pencil probe was utilised during testing. The pencil probe operates at a frequency of 50 kHz and was driven by a TSC AMIGO instrument.

To test the overall capability and performance of the ACFM system at high inspection speeds under controlled experimental conditions a special rotary test piece was manufactured, as shown in Figure 2.2. The material used for manufacturing the rotary test piece was a 0.9 wt % C steel to ensure that the microstructure, as well as the relative magnetic permeability and electrical conductivity, are similar to those exhibited by conventional 260 rail steel grade (typically 0.7-0.8 wt % C), with both steels having a predominantly pearlitic microstructure. The rotary test piece had a 230 mm diameter and was 60 mm thick, with a bore in the centre 190 mm in diameter and 50 mm deep.

Four transverse notches (2 x 2 mm and 2 x 4 mm deep with a flat profile) were spark eroded at the centre of the 20 mm wide rim of the sample. Each notch was 10 mm long and 0.5 mm wide. The sample was placed in a turning lathe capable of rotating the test piece between 1 and 3000 revolutions per minute (rpm). The rotational speed of one rpm for this experimental setup corresponded to the equivalent of a surface speed of 0.0405 km/h at the centre of the notch (i.e. 10 mm away from the edge of the rim). Hence at 3000 rpm the surface speed of the sample at the centre of the notches was 121.5 km/h. The ACFM probe was positioned opposite to the centre of the notches and at a 0° angle with reference to their surface orientation. The initial constant lift-off of the ACFM probe with regards to the surface of the rotating sample was 0.8 mm. Tests were carried out with a lift-off of up to 5 mm in order to evaluate the effect of increasing distance between the surface of the inspected sample and the probe on the ACFM signal.

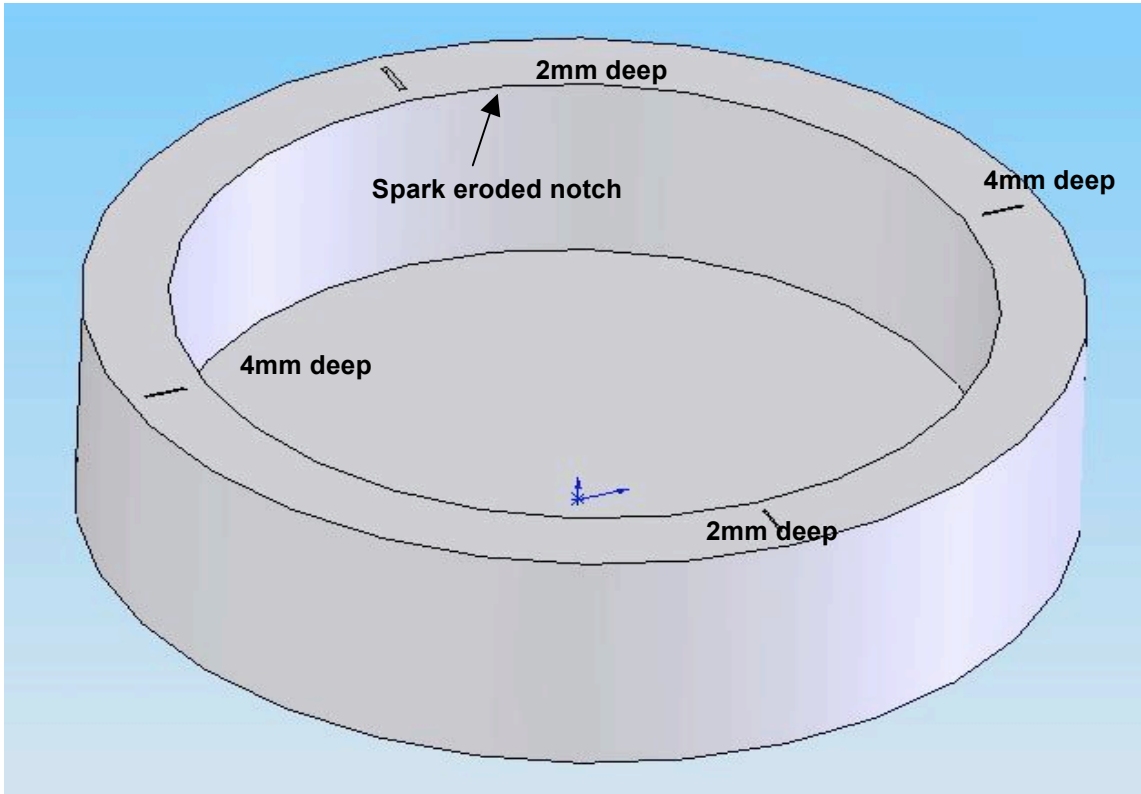


Figure 2.2 - Rotary test piece containing spark eroded notches

During experiments, the data were logged on the PC and then plotted using customised software. Further development of the software used is currently underway to enable plotting of the data in real time. The data logged during these tests were the ACFM probe signal (i.e. Analogue to Digital Conversion of probe voltage) with time. Data were collected for various speeds, starting from equivalent surface speeds of 4.05 km/h (at 100 rpm) up to 121.5 km/h (at 3000 rpm). Figures 2.3 and 2.4 show the ACFM signal response for the four notches at various speeds. Figure 2.5 shows the ACFM response with increasing lift-off at constant speed.

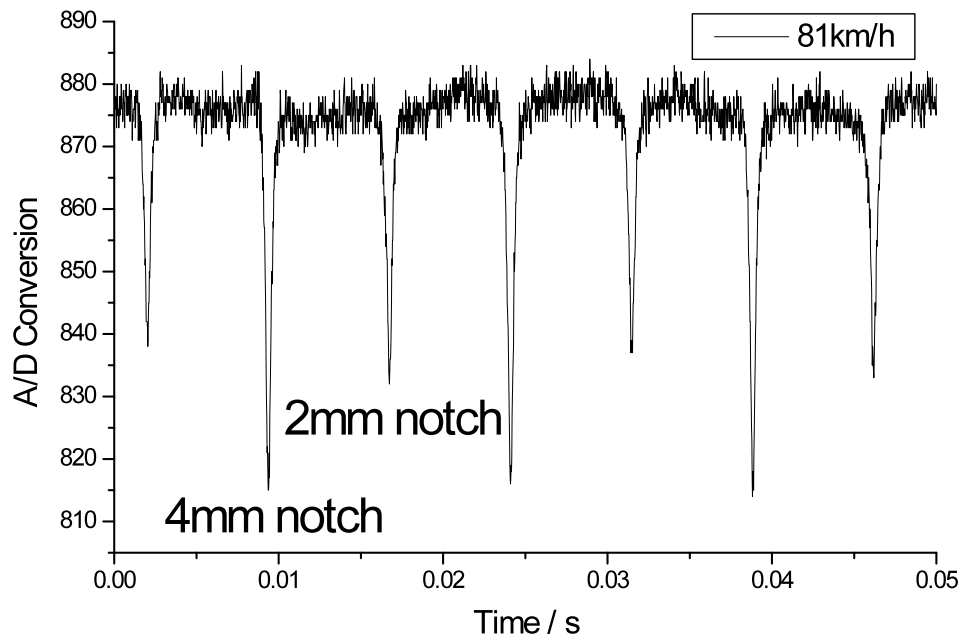


Figure 2.3 - ACFM data plot at 81 km/h with 0.8 mm probe lift-off

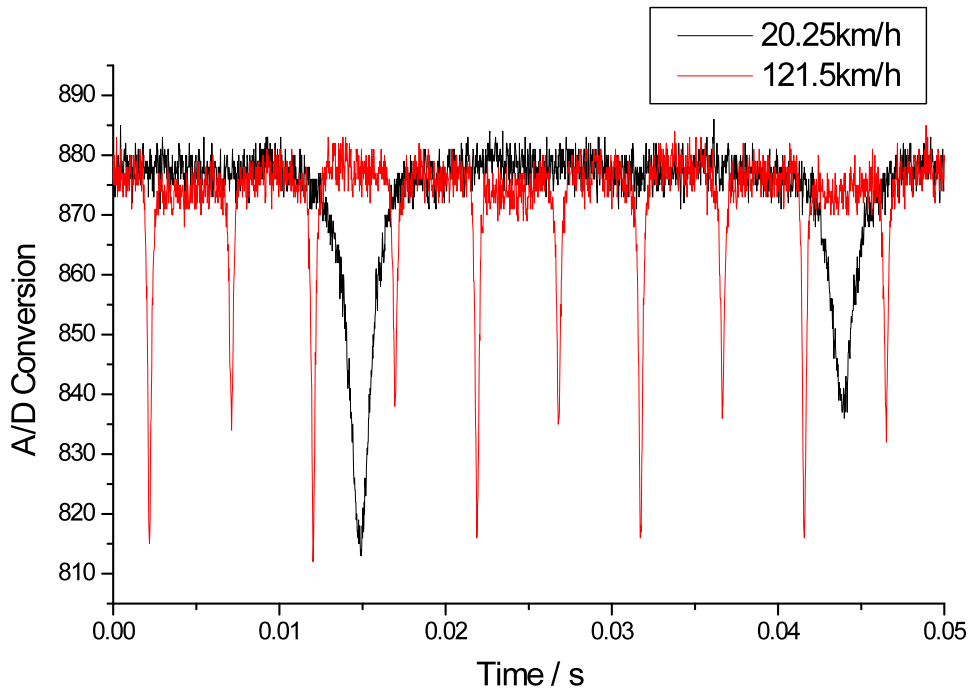


Figure 2.4 - ACFM data plots showing the resulting signals at 20.25 km/h and 121.5 km/h with 0.8 mm lift-off

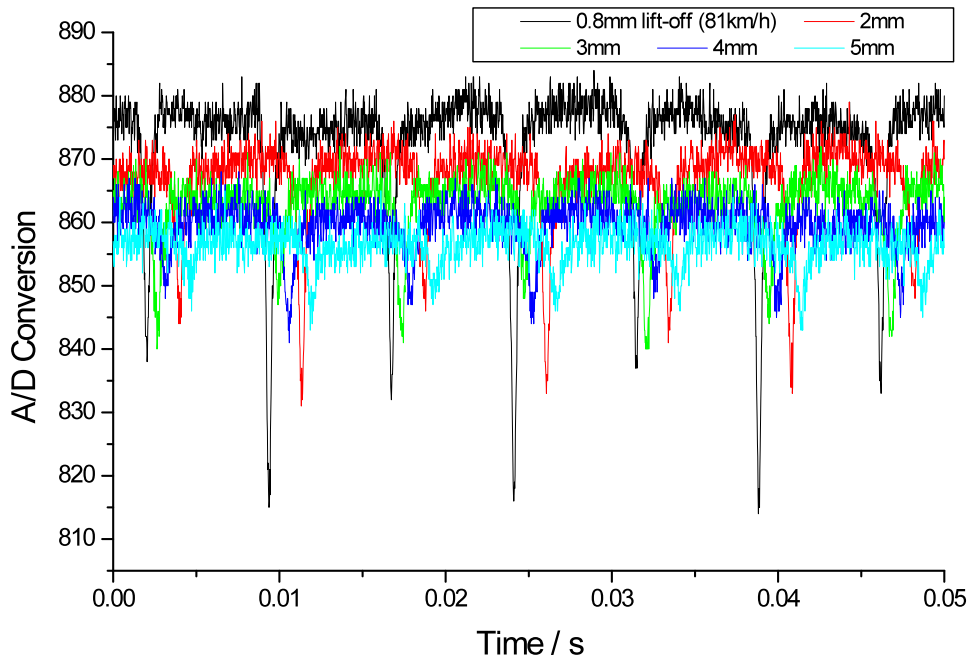


Figure 2.5 - ACFM signal with increasing lift-off

The ACFM tests carried out with increasing lift-offs (2 mm, 3 mm, 4 mm and 5 mm) at constant inspection speed showed a square reduction in the ACFM defect signal amplitude, as expected.

Manual tests without any lift-off were carried out on rails removed from service containing actual RCF cracking using a 5 kHz ACFM micro-pencil probe. Figure 2.6 shows the response for a rail without any defects present.

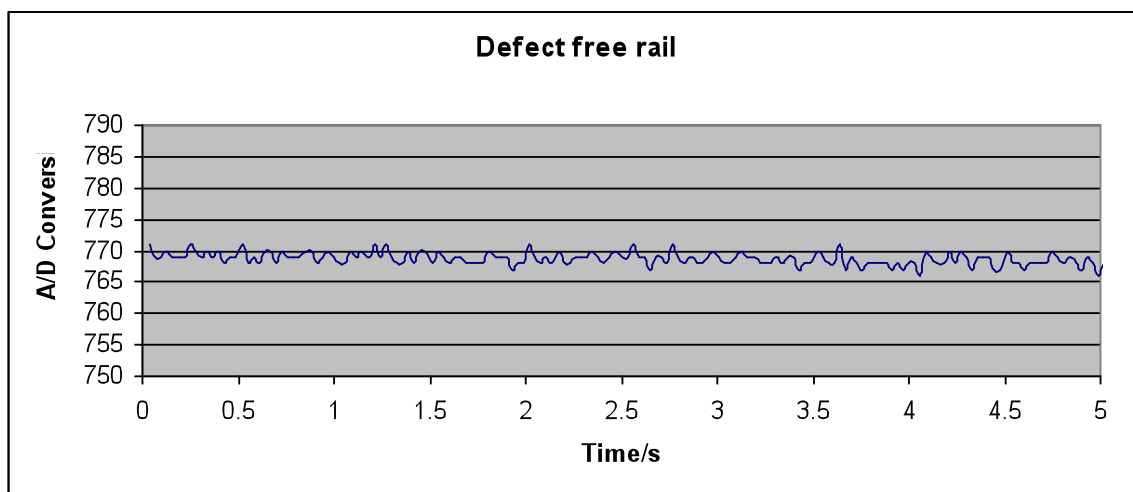


Figure 2.6 - Background ACFM signal versus time for a defect free rail

The diagram in Figure 2.7 shows the response obtained for a rail containing a dense population of moderate RCF cracks. From the signal no individual cracks can be resolved, however, it is clear that the damaged area gives rise to a varying ACFM signal, which can potentially be correlated to the severity of the damage.

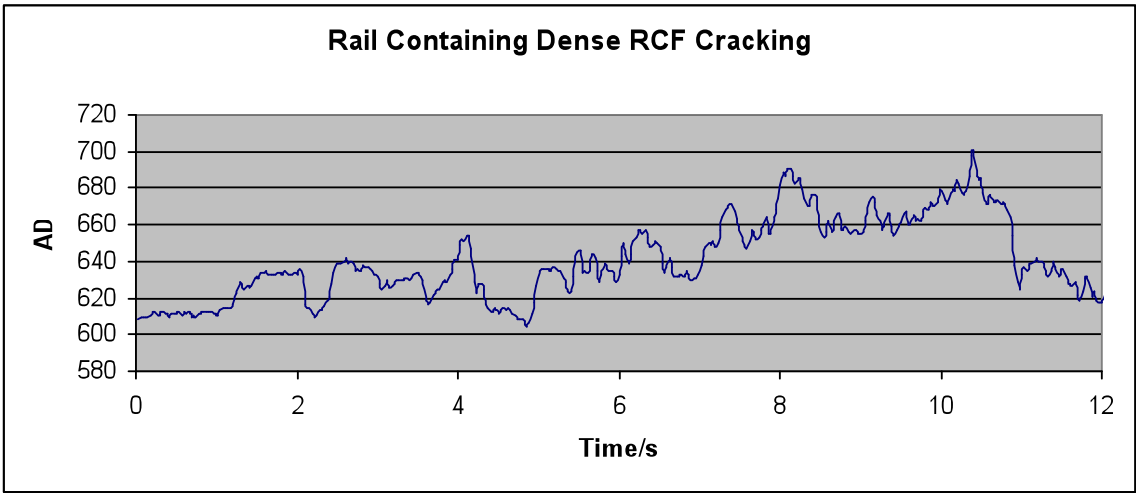


Figure 2.7 - ACFM signal versus time for a rail containing dense moderate RCF cracking

Figure 2.8 shows the ACFM response for a second rail containing a squat as well as a small number of moderate RCF cracks. The presence of a squat is identified by a rise in the ACFM sensor response, seen at the left hand-side of the diagram.

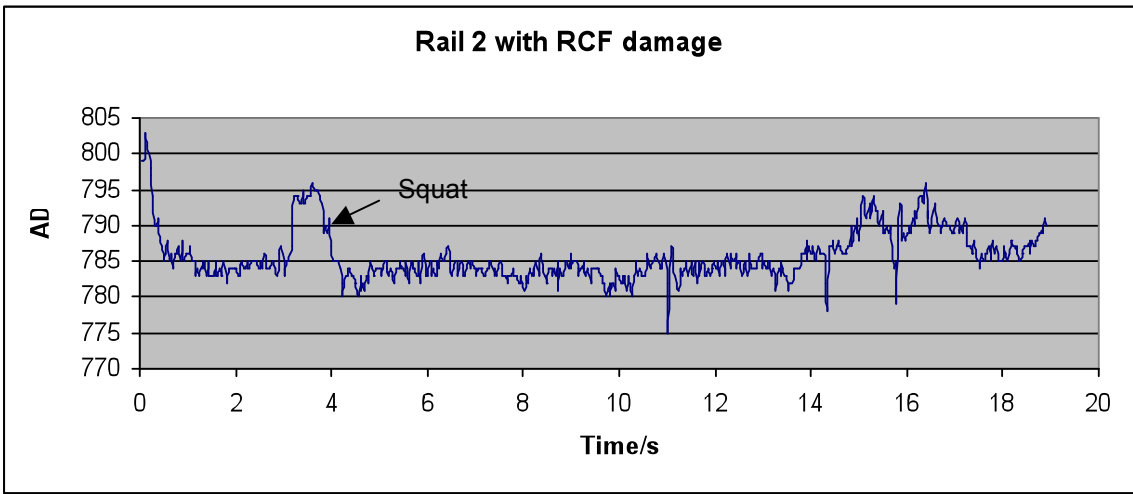


Figure 2.8 - ACFM signal versus time for a rail containing dense moderate RCF cracking

2.3 On-site Testing

Initially, manual ACFM tests (i.e. without the use of the trolley) were carried out. Figure 2.9 shows the ACFM response obtained during manual rail inspection at the Swindon test site over an area of 200 mm. Some small RCF cracks can be identified.

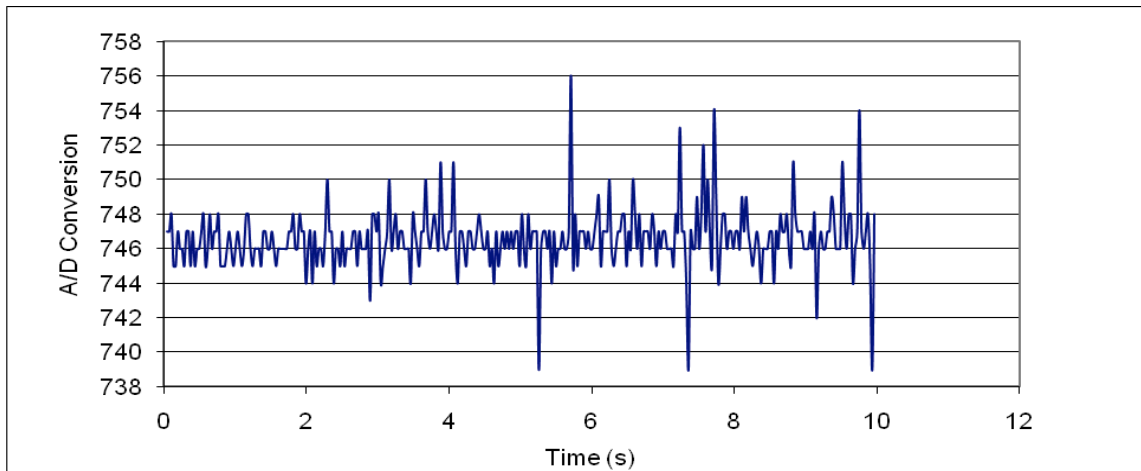


Figure 2.9 - Manual ACFM inspection response from Swindon test site

The photos in Figure 2.10 show the trolley equipped with the ACFM and EMAT sensors during the Swindon test trials.



Figure 2.10 - Swindon test site and trolley equipped with EMAT and ACFM sensors

The trolley was initially pushed along the rail section containing light RCF cracks. The speed of inspection was approximately 0.2 m/s. The top diagram in Figure 2.11 shows the ACFM response obtained for the entire length of the rail section.

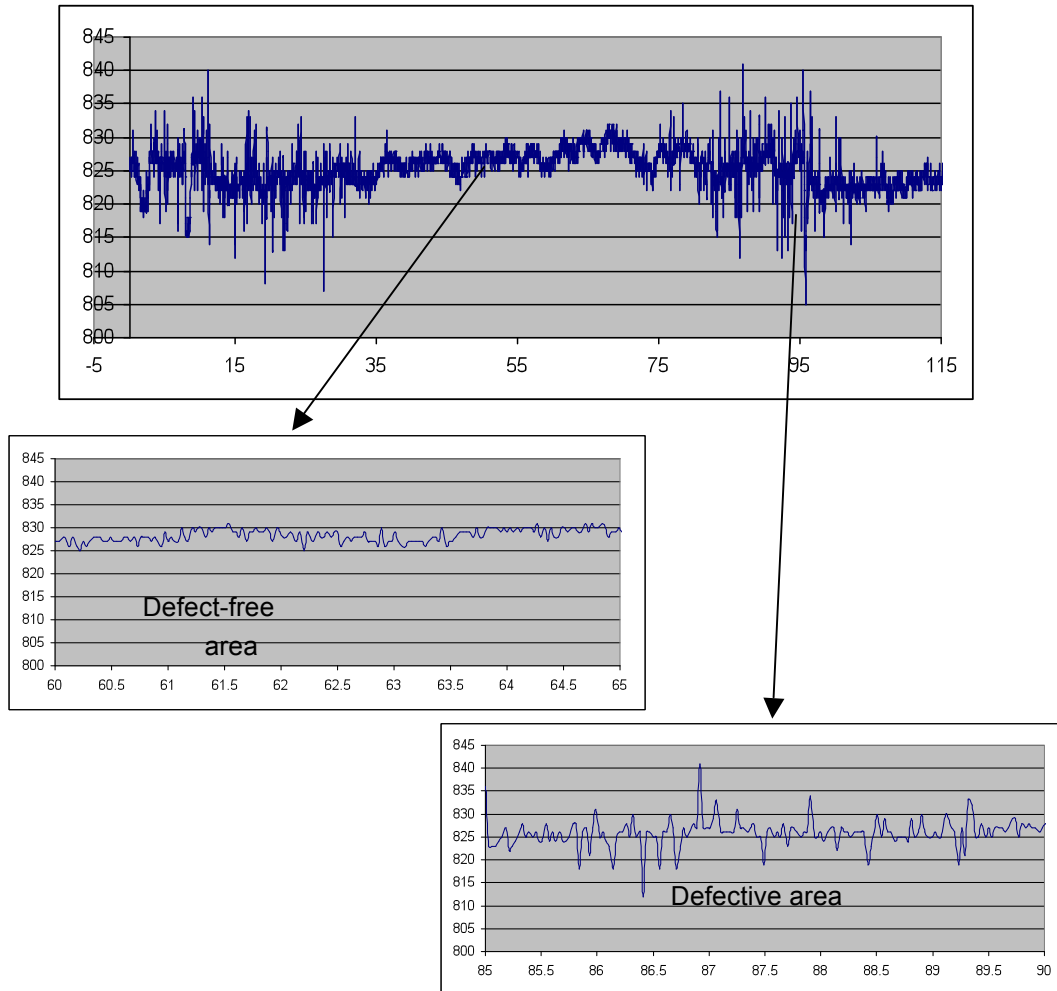


Figure 2.11 - Trolley inspection results for the rail section identified to contain light RCF cracking

The inspection of the light RCF section revealed that there were RCF cracks present, albeit not throughout the entire length of the rail. It also appeared that certain areas potentially contained small clusters of RCF cracks. The second diagram in Figure 2.11 shows the ACFM signal over an area of the inspected rail section containing no defects whilst the third (bottom) diagram shows the ACFM response over an area containing RCF cracking.

Similarly, Figure 2.12 shows the ACFM response for the inspected rail section identified to contain moderate RCF cracks.

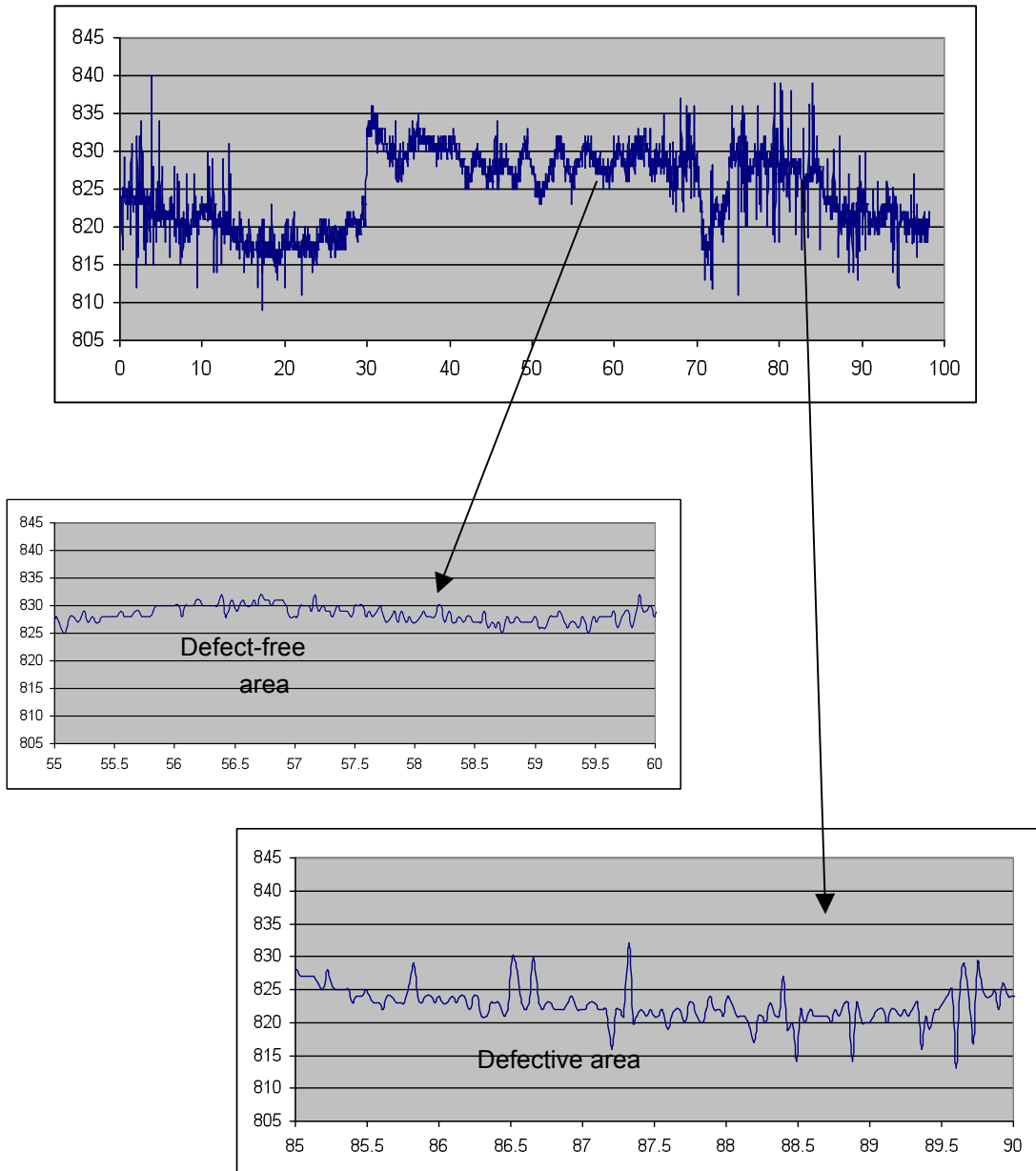


Figure 2.12 - ACFM trolley inspection results for the rail section identified to contain moderate RCF cracking

2.4 Conclusions

The inspection of the moderate RCF section showed that there were RCF cracks present with a similar, but slightly more dense, distribution as compared to the light-RCF rail section.

Although it is not currently possible to quantify the cracks detected from the results, it can be seen that the ACFM sensor was capable of successfully detecting the damage present on the rails. It is also possible to qualitatively determine the extent of the damage present on the rail sections inspected.

Further developments are underway to enable a more quantitative evaluation of RCF damage on rails using ACFM sensor technology. Further work will be undertaken in the FP7 funded INTERAIL project.

3. Detection of Surface Defects by Image Analysis

3.1 Background

Corus, as part of a consortium, have previously undertaken a project on detection of defects by image capture and intelligent analysis [11]. The work that has been carried out within the Innotrack project has been to demonstrate that the system is applicable to main line railways. The ultimate aim for such systems is to mount equipment on inspection or service vehicles and monitor the surface growth of defects. Rail defect imaging cameras can also be combined with other current, or future, detection systems to provide more information about the defects, which will allow more effective planning of maintenance. The rail inspection system can also be combined with other cameras to allow inspection of other infrastructure features, such as clips, sleepers, switches and crossings etc. to be monitored automatically.

The initial development has produced a camera and lighting system, mounted onto a trolley that is pushed by hand as shown in Figure 3.1. The trolley gathers images for analysis and demonstrates the feasibility of the approach. The imaging system uses a video camera with a resolution of 80 μm and an image capture rate of 30 frames per second. The illumination used is a high power strobe system built into a specially designed diffusing enclosure. The images are stored on a computer and analysed at a later date. The speed of image capture is walking pace but a feasibility study has been carried out to determine the maximum operational conditions for a vehicle mounted system. With the current camera a maximum speed of 20km/h is possible, faster speeds would be possible with multiple cameras.

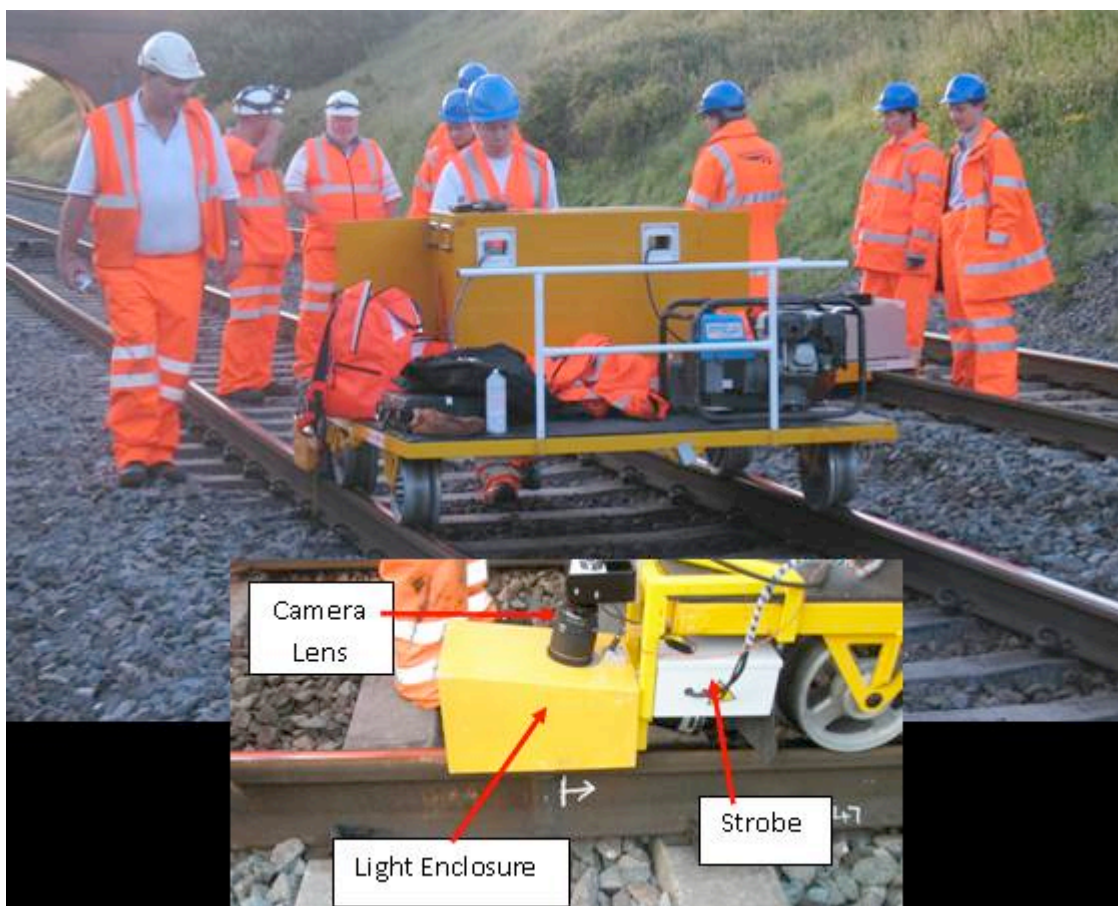


Figure 3.1 - Image capture trolley

Images were taken on both 'up' and 'down' lines at locations where rolling contact fatigue (RCF) cracks have been reported. At the same time, conventional rail inspection techniques, such as Magnetic Particle Inspection (MPI), were used to allow comparison with the images taken by the trolley.

Software has been developed to enable analysis of the images taken by the trolley to be carried out. This software allows detection and characterisation of the running band. Analysis of the running band, especially deviations in width, can detect welds, squats and wheel burns. A second part of the software uses edge detection algorithms to look for RCF defects.

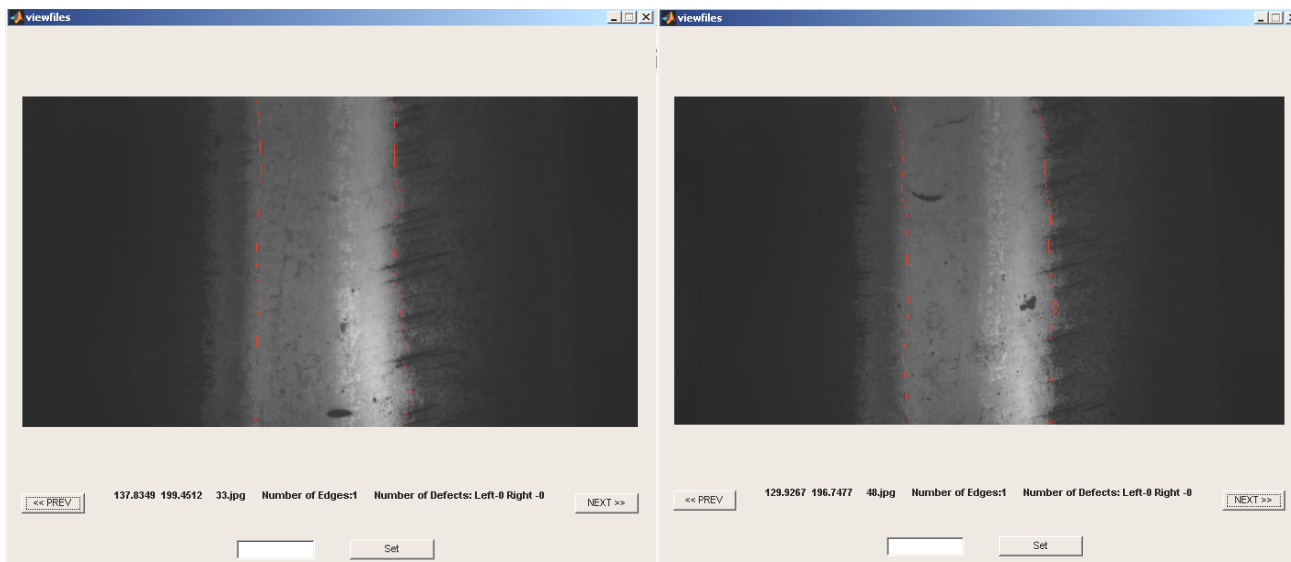


Figure 3.2 - Image analysis software detecting running bands

The software was used on several images to detect running bands, as shown by the red lines in Figure 3.2. This demonstrates that it is close to the actual observed position. Unfortunately, the lighting of the camera was suboptimal and therefore only the centre of the rail is visible in the pictures, with loss of resolution near to the edges of the rail head. In the section of track examined there were no significant deviations in the running band that indicated the presence of dipped welds or squats.

Problems with the rail defect identification software meant that it was unable to identify any defects. One of the reasons for this is that the site had recently been ground, resulting in extensive residual grinding marks, as shown in Figure 3.3.



Figure 3.3 - Digital photograph of rail condition

The grinding relocated the running band from the gauge corner to the centre of the rail head, resulting in any RCF cracks present being disguised by the residual grinding marks. The suboptimal trolley set up also made the identification of defects difficult. Magnetic particle inspection (MPI) of the rail where the RCF was thought to be most severe revealed that only a few small cracks were present, as those reported by NR had probably been removed by grinding.

Some surface defects that were thought unlikely to be RCF were observed within the running band, an example is given in Figure 3.4. The software was unable to find these isolated defects as the system is optimised to find RCF and these defects were at a different orientation.

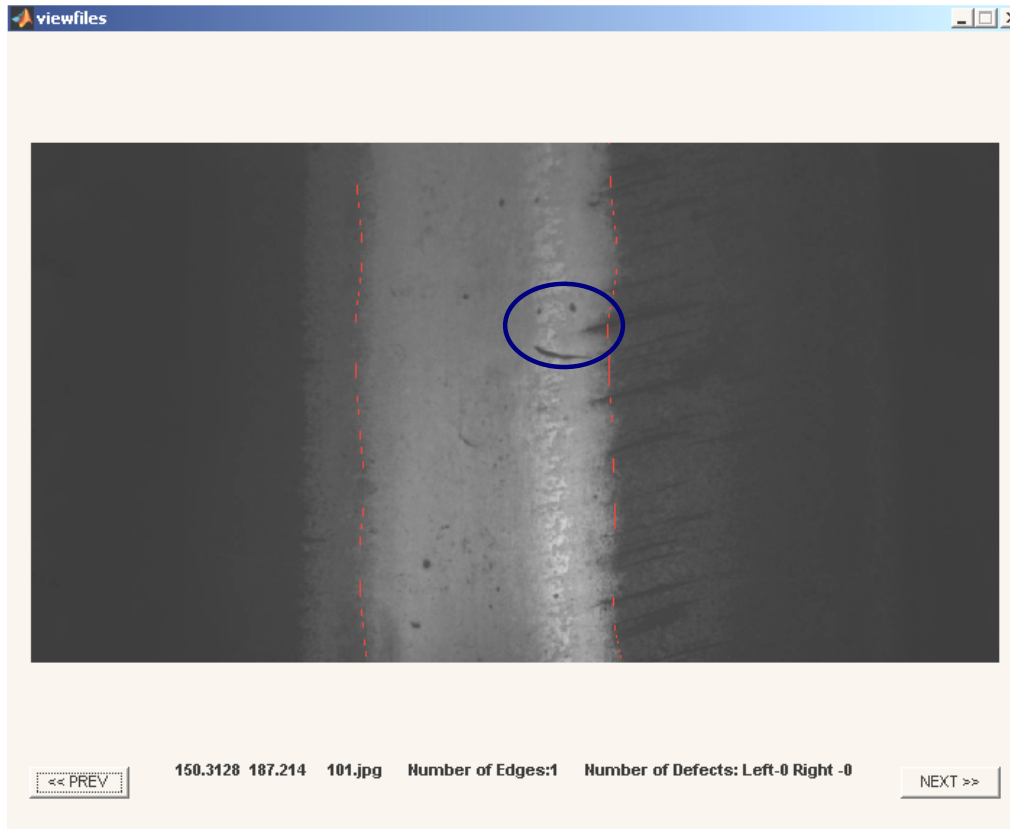


Figure 3.4 - Image from trolley of surface defect in running band

A detailed investigation of these defects was undertaken during the site visit using Alternating Current Potential Difference (ACPD) equipment, which had been calibrated for grade R220 rail, the defect was found to be approximately 0.1mm deep.



Figure 3.5 - Digital photograph of surface defect.

3.3 Conclusions

The testing of the image analysis trolley on mixed traffic railways has demonstrated that:

- Deviations in the running band and defects within it are readily observable from a trolley mounted camera;
- The presence of residual grinding marks makes it difficult to detect defects away from the running band;
- The image quality from the current camera systems is suboptimal, especially as it is unable to capture images at speeds of greater than 20 km/h;
- The current software is unable to detect defects within the running band but can detect the width of the running band.

To overcome these difficulties Corus along with Manchester Metropolitan University is undertaking further work on image analysis of rails within the FP7 project PM 'n' IDEA. This concentrates on light rail and metro systems but will ultimately be usable on mixed traffic systems. The improvements include:

- The use of a camera and lighting system that is able to give higher resolution images and which can be used at higher speeds. The camera will also be fitted to a light rail vehicles to demonstrate the feasibility of using such systems in service;
- The development of software, which is more intelligent than the current versions. This will include using a range of image analysis techniques, rather than just edge detection, to be able to look for a range of defects that are present in varied orientations.
- Inspection of components, other than just the rail, within 0.5m of the centre of the rail head. To allow a more comprehensive system that allows further automation of track inspection.

The results of this development will be reported when complete within the FP7, PM 'n' IDEA project.

4. Inspection of Surface Defects by EMATs

4.1 Background

The University of Warwick have developed a 'pitch-catch' low frequency wideband Rayleigh wave EMAT system that has been used for detection and depth gauging of transverse cracks in the rail head, such as gauge corner cracking. The ultrasonic waves that are used in this technique are a type of guided wave mode that is very similar in characteristics to a classical Rayleigh surface wave. These waves propagate along the surface of the rail penetrating down to a depth approximately equal to their wavelength, between 2 to 15 mm. The surface wave that is generated is wideband, containing a range of frequencies in one single pulse. The depth of a crack can be estimated by measuring the relative amount of the surface wave at a particular frequency that passes underneath the crack, compared to the frequency content of a wave that has propagated along a defect free region. The set-up is shown in the schematic diagram of Figure 4.1. Preliminary measurements indicate that this new ultrasonic system also has the potential to assess the condition of the combined microstructure and stress state around the rail head, potentially identifying precursors to crack formation.

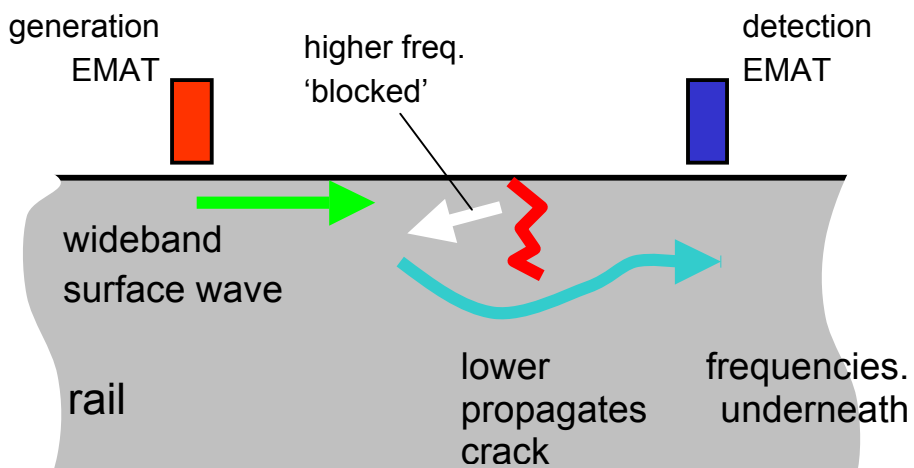


Figure 4.1 - Schematic diagram to illustrate the pitch-catch surface wave measurement for crack detection (N.B. the generation and detection EMAT are fixed relative to each other, thus the pair move together)

4.2 On-Site Testing

The transducers were attached to a hand-pushed trolley as shown below in the schematic diagram of Figure 4.2, and the supporting electronics were housed in a weather proof box on the platform of the trolley.

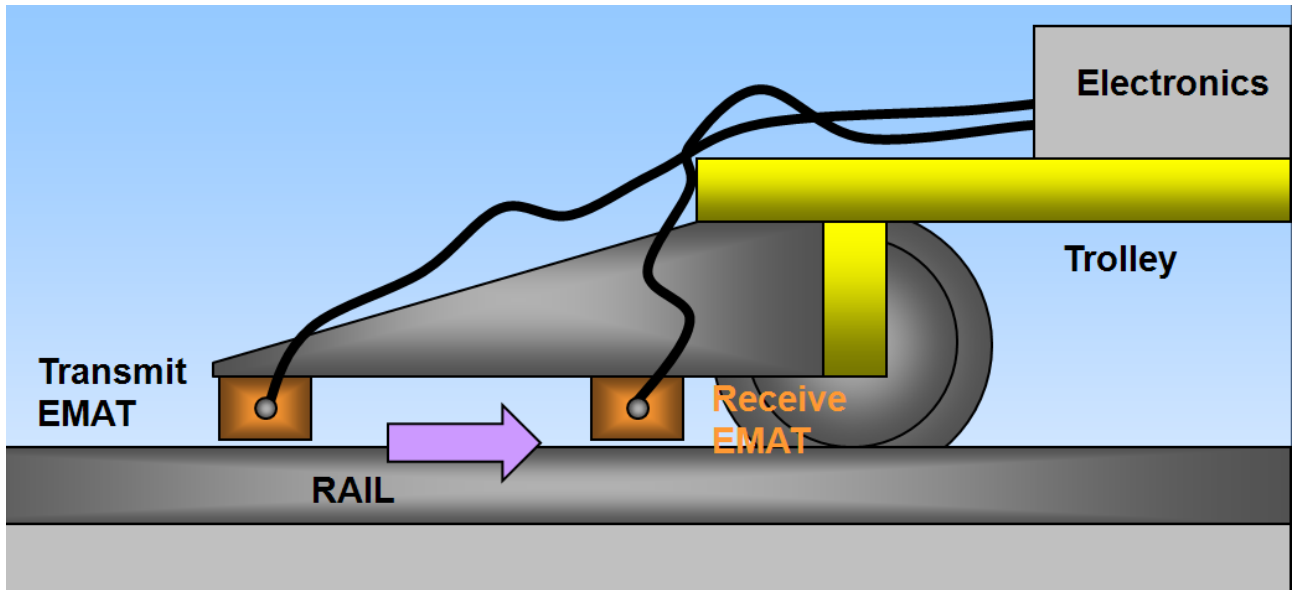


Figure 4.2 - Schematic diagram to illustrate the implementation and attachment of the EMAT system to the hand-pushed trolley

Typical waveforms recorded on areas of high and moderate RCF are shown below in Figure 4.3a, together with the associated Fast Fourier Transform (FFT) of the same data in Figure 4.3b.

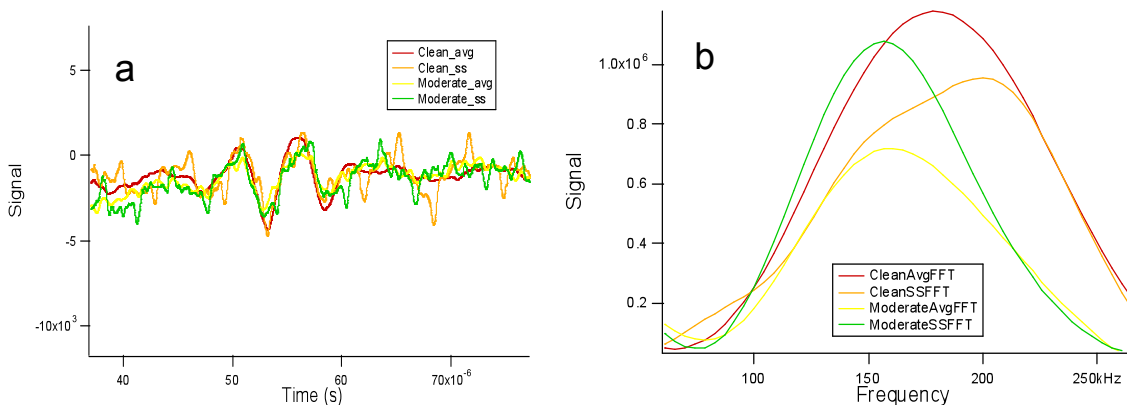


Figure 4.3 - time domain waveforms: (a) show evidence for some noise pick-up, (b) the FFT of these waveforms showing the frequency region with higher RCF that has a quantifiably lower frequency content

As expected, the region with higher RCF appears to have higher attenuation of the higher frequency components, as lower frequency components are contained within a thicker region of the surface layer of the rail and pass under the cracks more readily.

The trolley was passed over regions of clear, light and medium RCF as defined by Network Rail. In order to view the data more easily, the time domain waveforms, such as those shown in Figure 4.3a, have their amplitudes assigned a colour coding and are plotted side-by-side in what is commonly referred to as a B-scan. The quantitative information is of course preserved, and the data is presented in this way simply to aid interpretation. A similar procedure is used on the frequency domain data, in which the FFTs are also amplitude colour coded and stacked side-by-side. The results of a typical scan are shown in Figure 4.4. Note that the horizontal scale is not directly linked to position as the equipment was triggering at a fixed repetition rate. Future tests should include a means of recording position using a shaft encoder or similar.

Indicative of a region
of higher defect
density

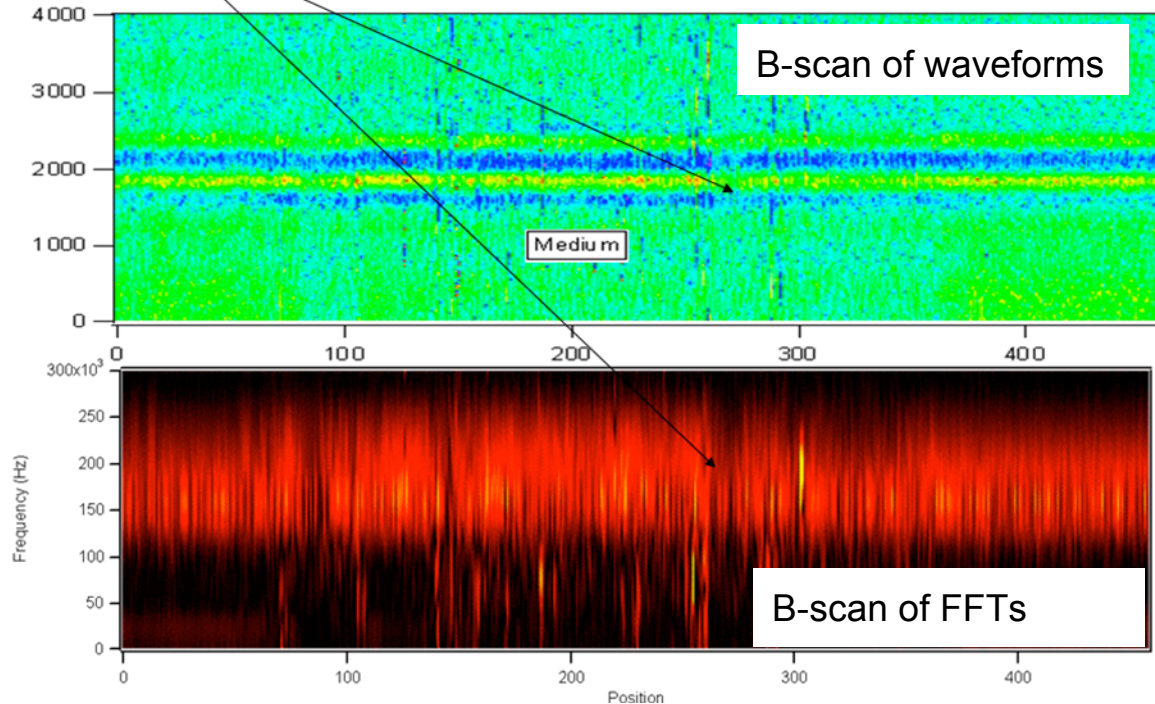


Figure 4.4 - The time domain waveforms and FFTs stacked side-by-side where the horizontal axes are related to the position along the rail

There is evidence in the time domain waveforms and the FFTs that electrical noise spikes are present in the data. The source of these is as yet unknown, but this noise can be eliminated either by improvement of equipment shielding during tests and/or signal processing.

4.3 Conclusions

There were many other scans of such data, as shown in Figure 4.4, but they are not presented here, as without a detailed knowledge of the defects in the rail it is not possible to correlate the data to any known defects. This cannot be done retrospectively, as the position of the EMATs was not accurately recorded relative to a reference point. The data clearly shows that there appear to be regions where both the amplitude and high frequency content of the surface waves fall, which would be consistent with the presence of defects. No major falls in amplitude appear to have been recorded, suggesting that there are no very deep (>20 mm) defects in the sections of track that were tested.

Future work includes the construction of an array of detectors rather than the use of just one detector. This should increase the ability to detect cracks shorter than 10 mm in length. A new design of EMAT with lower noise susceptibility has been demonstrated, and this design will be incorporated into future tests. When further tests are undertaken, a more quantitative measurement of the defects in the rail and their position will be required, together with an accurate measurement of the position where the data was recorded on the trolley based rig.

5. Conclusions

As expected, a number of difficulties were encountered when taking equipment which had previously been lab based into the field for testing. The ACFM and EMAT approaches showed potential to identify and characterise RCF defects. The accuracy of the results was compromised as only general data was available about the particular defects being inspected and the precision of the trolley location. Further work will be carried out in a variety of further projects.

For ACFM, the inspection of the moderate RCF section showed that there were RCF cracks present with a similar but slightly more dense distribution as compared to the light RCF rail section.

Although it is not currently possible to quantify the cracks detected from the results, it can be seen that the ACFM sensor was capable of successfully detecting the damage present on the rails. It is also possible to qualitatively determine the extent of the damage present on the rail sections inspected.

Further developments are underway to enable a more quantitative evaluation of RCF damage on rails using ACFM sensor technology. Further work will be undertaken in the FP7 funded INTERAIL project.

The testing of the image analysis trolley on mixed traffic railways demonstrated that:

- Deviations in running band and defects within it are readily observable from a trolley mounted camera;
- The presence of residual grinding marks makes it difficult to detect defects away from the running band;
- The image quality from the current camera systems is suboptimal, especially as it is unable to capture images at speeds of greater than 20 km/h;
- The current software is unable to detect defects within the running band but can detect the width of the running band.

To overcome these difficulties, Corus along with Manchester Metropolitan University is undertaking further work on image analysis of rails within the FP7 project PM 'n' IDEA, concentrating on light rail and metro systems, which will ultimately be usable on mixed traffic systems. The improvements include:

- The use of a camera and lighting system that is able to give higher resolution images and be used at higher speeds. The camera will also be fitted to light rail vehicles to demonstrate the feasibility of using such systems in service;
- The development of software which is more intelligent than current versions. This will include using a range of image analysis techniques, rather than just edge detection, to be able to look for a range of defects that are present in a range of orientations.
- Inspection of components, other than just the rail, within 0.5m of the centre of the rail head. To allow a more comprehensive system that allows further automation of track inspection.

The results of this development will be reported when complete within the PM 'n' IDEA project.

The EMATs data clearly shows that there appear to be regions where both the amplitude and high frequency content of the surface waves fall, which would be consistent with the presence of defects. No major falls in amplitude appear to have been recorded, suggesting that there are no very deep (>20 mm) defects in the sections of track that were tested.

Future work includes the construction of an array of detectors rather than the use of just one detector. This should increase the ability to detect cracks shorter than 10 mm in length. A new design of EMAT with lower noise susceptibility has been demonstrated and this design will be incorporated into future tests. When further tests are undertaken, a more quantitative measurement of the defects in the rail and their position will

be required, together with an accurate measurement of position of where the data was recorded on the trolley based rig.

6. References

- [1A] D4.1.4 *Rail Degradation Algorithms*, Lead partners: Corus and voestalpine, Inntrack Deliverable, 2009
- [1B] D4.3.6 *Characterisation of Microstructural Deformation as a function of Rail Grade*, Lead partner: Corus, Inntrack Deliverable, 2009
- [1C] Rolling contact fatigue in rails: a guide to understanding and practice [“The Blue Book”], Railtrack PLC., RT/PWG/001 Issue 1, February 2001.
- [2] Lugg, M. C., Shang, H. M., Collins, R., Michael, D. H. The measurement of surface crack inclination in metals using AC electric fields, *J. Phys. D: Appl. Phys.*, Vol 21, pp. 1814-1821, 1988.
- [3] Topp, D., Smith, M. Application of the ACFM Inspection Method to Rail and Rail Vehicles, In the Proceedings of ENCDT 2005.
- [4] Lugg, M., Topp, D. Recent developments and applications of the ACFM inspection method and ACSM stress measurement method, In the Proceedings of ECNDT 2006, Berlin, German.
- [5] Papaalias, M., Roberts, C., Davis, C., Blakeley, M. Lugg. Further developments in high-speed detection of rail rolling contact fatigue using ACFM techniques, Non-Destructive Testing 2009 Conference, Blackpool, UK, September 2009.
- [6] Girardi, L., Plu, J., Blakeley, B., Bredif, P., Davis, C., Lugg, M., Papaalias, M., Roberts, C., INNTRACK SP4.4 – Detection of Rolling Contact Fatigue in Rails Using Electromagnetic and Ultrasonic Phased-Array Inspection Techniques, 8th International Conference on Contact Mechanics and Wear of Rail/Wheel Systems, Firenze, Italy, September 15-18,2009.
- [7] Papaalias, M., Roberts, C., Davis, C., Blakeley, B., Lugg, M. Detection and quantification of rail contact fatigue cracks in rails using ACFM technology, *Journal of the British Institute of Non-Destructive Testing (Insight)*, Number 7, July 2009.
- [8] Papaalias, M., Lugg, M., Roberts, C., Davis, C. High-Speed inspection of rails using ACFM technology, *Journal of NDT&E International*, Vol. 42, Number 4, June 2009.
- [9] Papaalias, M., Roberts, C., Davis, C. A review on non-destructive evaluation of rails: state of the art and future development, *I. Mech. E. Proceedings, Journal of Rail and Rapid Transit – Part F, Invited Review Paper*, Vol. 222, Number F4, December 2008.
- [10] Papaalias, M., Roberts, C., Davis, C., Lugg, M., Smith, M. Detection and quantification of rail contact fatigue cracks in rails using ACFM technology, *Journal of the British Institute of Non-Destructive Testing (Insight)*, Number 7, July 2008.
- [11] Autonomous Rail Track Inspection using Vision Based System, Singh, M. Singh, S. Jaiswal, J. Hempshall, J., Proceedings of the 2006 IEEE International Conference on Computational Intelligence for Homeland Security and Personal Safety, Alexandria, VA, 16-17 Oct. 2006